Supporting Information

Towal et al. 10.1073/pnas.1304429110

SI Computational Model

Probabilistic Gaze Transitions. In the Krajbich and Rangel version of this model published in 2010 and 2011, the transitions between one item being fixated on and another item being fixated on were determined empirically from the subject data (1, 2). Thus, these transitions occurred instantaneously at the times when subjects changed their fixation location. Furthermore, in the Krajbich and Rangel model, their simulations were performed by integrating the drift–diffusion model (DDM) process 50 times, and thus in each iteration, the process had one specific value at each time when the transition was made (Fig. S1*A*). Importantly, in the version of the model published in 2012, the transitions were considered to be probabilistic, but were still based on the exogenously measured fixation statistics and not modeled in any way (3).

Here, we make two improvements to this method. First, we have a probabilistic expression for the location of the process in time, meaning that at any particular time the location of the process can be described as a Gaussian with a known mean and SD (Fig. S1*B*). Second, we are modeling the gaze trajectories and we have a probabilistic model of when these transitions will occur. Thus, our transitions will not occur at one specific time, but will instead have some probability of occurring as a function of time, described by Eq. **8** (Fig. S1*C*).

The consequence of this probabilistic approach is that at each gaze transition we must start the new DDM process from a probabilistic location rather than a single point (Fig. S1*C*). To accomplish this, we simply take the $p(y_i|t)$ from Eq. **12** at each time t and scale it by $\mathbf{f}_{i,j}(t)$ for each transition:

$$\forall t : \mathbf{f}_{i,j}(t) \times p(y_i|t). \qquad \textbf{[S1]}$$

Conditional Choice Model Example. Fig. S2 shows an example of the conditional choice model for one gaze trajectory across the example shown in the main text in Fig. 1. The decision process for each item is shown separately in the four columns. The items are ordered in the sequence they were fixated on from left to right. In Fig. S2, *Upper*, we show the probabilistic extent of the absolute decision process $y_j(t)$.

Because the Chips Ahoy were fixated on first in the sequence for 160 ms, the drift of the associated accumulator is highest for the first 160 ms, and then the drift decreases for the remainder of the trial. The same can be seen for the other four items across Fig. S2, *Upper*; namely that when the item is fixated on, the drift is higher than when it is not.

Because the conditional choice model considers the relative value of the accumulator and not the absolute value, we also show the relative value of the accumulators, $Y_j(t)$ in Fig. S2, *Lower*. To calculate the relative accumulation, a max-vs.-next operation is performed as described in the main text. Specifically, for each point in time, there are four Gaussians describing the location of the absolute accumulators for each item. At each point in time, we compute the difference between the Gaussians for one process, say the Sun Chips in Fig. S2, by subtracting a probabilistic estimate of where the next-highest process is. Finding the "next highest" process from three overlapping Gaussians is solved in much the same way as finding the probability that each gaze accumulator will cross the threshold first (Eqs. **6** and **7**, main text). Specifically, we start by finding the portion of each Gaussian that is higher than the rest by multiplying the Gaussian of interest by the cumulative distribution function of the other two Gaussians. The part of the Gaussian of interest that survives this multiplication is the part of that process that is higher than the rest. This is repeated for all three Gaussians. The results of this operation are then summed, to produce a combined probability distribution function that describes all of the locations that the other three process could occupy and be considered the "next highest". This probability density function is then subtracted from the Gaussian for the Sun Chips, say, to produce the relative $Y_j(t)$ at a particular point in time. This process is repeated for all processes and time points. Fig. S2, *Lower* shows the result of this computation for this example.

Intuitively, the result of this computation is that when the absolute accumulation for an item is higher than that for any other item, the relative accumulation increases, and vice versa. For the case of the second item fixated on (the Chewy Sweet Tarts), the depressed drift in the first 160 ms causes this process to have a lower $y_j(t)$ than the next-highest process, which results in a negative slope for the $Y_j(t)$ for the Chewy Sweet Tarts during the first 160 ms. During the second fixation, however, because the Chewy Sweet Tarts are fixated and their $y_j(t)$ is higher than that of the rest of the accumulators, the max-vs.-next operation yields an increasing $Y_j(t)$. During the second fixation, the second relative accumulation process has a small probability of crossing the threshold. This is shown as the $p(n|t_k)$ displayed above the threshold. Importantly, although some instances of this process may cross the threshold during the second fixation, even during the third fixation there is a chance that the process will cross the threshold, indicated as the middle process in Fig. S2, *Lower*. Of course, there is also the possibility that the process will never cross the threshold, e.g., the bottom process in Fig. S2, *Lower*.

Calculation of the Area Under the Receiver–Operator Characteristic Curve. The procedure for calculating the receiver–operator characteristic curve is described in the text and is illustrated here in Fig. S5.

1. Krajbich I, Armel C, Rangel A (2010) Visual fixations and the computation and comparison of value in simple choice. *Nat Neurosci* 13(10):1292–1298.
2. Krajbich I, Rangel A (2011) Multialternative drift-diffusion model predicts the relationship between visual fixations and choice in value-based decisions. *Proc Natl Acad Sci USA* 108(33):13852–13857.
3. Krajbich I, Lu D, Camerer C, Rangel A (2012) The attentional drift-diffusion model extends to simple purchasing decisions. *Front Psychol* 3:193.

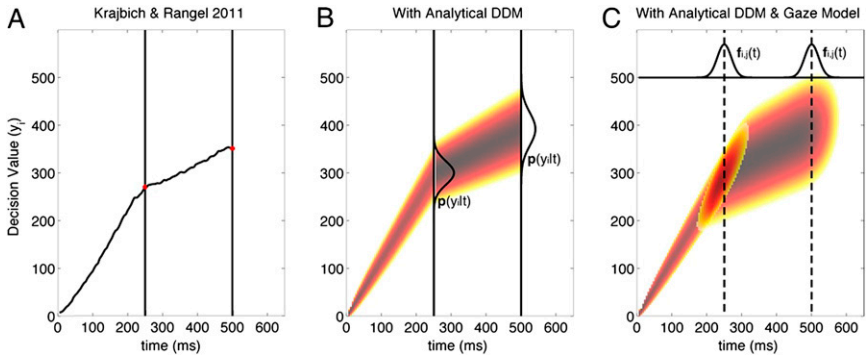

Fig. S1. Comparison of how gaze transitions are calculated. (*A*) Illustration of the gaze transition definition from refs. 1 and 2. Vertical lines indicate gaze transition times. (*B*) An illustration of the distribution of the decision variable at singular transition times. (*C*) Illustration of the probabilistic transition times used here. In all panels, darker regions indicate a higher probability of the process occupying a particular value at a particular time. *y*-axis numbers are arbitrary.

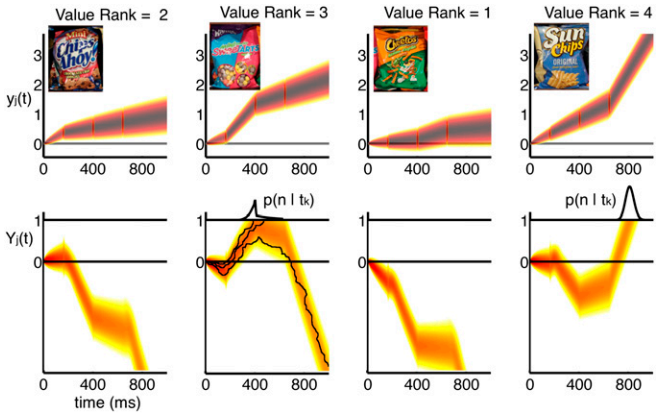

Fig. S2. Illustration of the conditional choice model. (*Upper*) The decision variable, $y_j(t)$, as it evolves in time with four fixations. Items are fixated on in the order shown from left to right (value ranks: 2, 3, 1, 4). Leftmost panel shows the decision variable for the item with value rank 2 that was fixated first. Darker regions indicate a higher probability of the decision variable occupying that value at a particular time. Rounded areas highlight the points when fixations occur (see Fig. S1). (*Lower*) The upper solid horizontal black line shows the probability that the relative decision variable, $Y_j(t)$ has crossed the threshold given this particular gaze trajectory. The lower solid horizontal black line shows the relative decision variable $Y_j(t)$ as it evolves for each item. As in the *Upper* section, darker regions indicate a higher probability of the relative decision variable occupying that value at a particular time. In the second panel, we also show three example instantiations of this process, one that hits the threshold early, one that hits the threshold even after the process is generally decreasing, and one that does not hit the threshold (black lines). In this example the item with value rank 4 is the most likely to be chosen because it has the largest probability of crossing the threshold early in the trial. However, there is a small probability that the item with value rank of 3 may cross the threshold first.

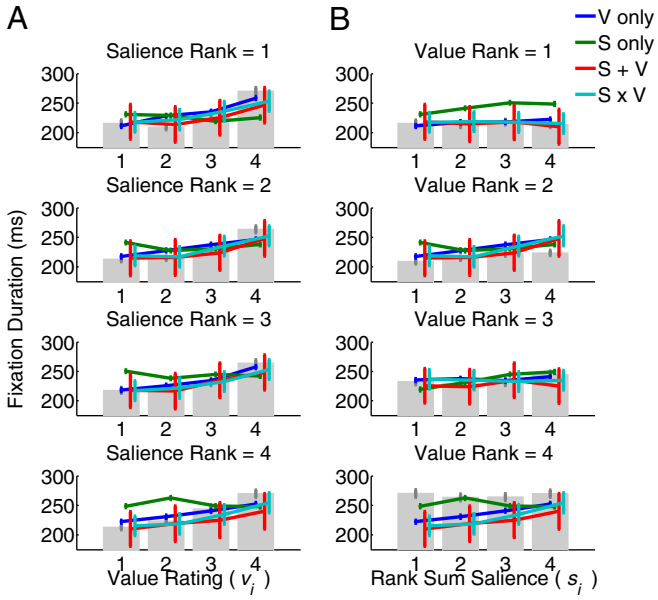

Fig. S3. Modeled vs. actual gaze broken down by all salience–value combinations. (*A*) Fixation durations as a function of value for each saliency rank. (*B*) Fixation durations as a function of saliency for each value rank. Gray bars indicate actual fixation durations. Model results are shown as colored lines (mean ± SEM) and offset on the *x* axis to facilitate comparison.

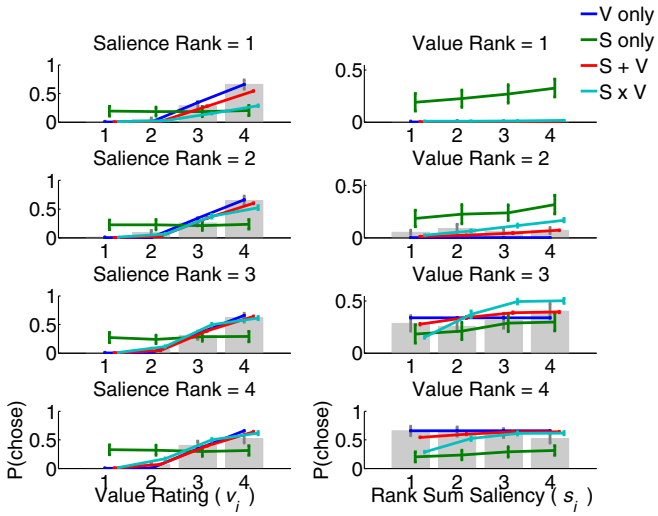

Fig. S4. Choice probabilities as a function of all salience–value combinations. Gray bars and error bars indicate $p(n)$ for our data. Model results are shown as colored lines (mean ± SEM) and are offset on the *x* axis to facilitate comparison.

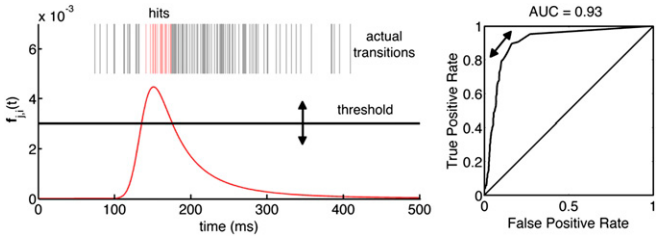

Fig. S5. Calculation of the AUC. (*Left*) Vertical lines indicate the measured transition times from item 1 to item 2 for one subject while looking at one *sv* combination. The red curve below the transition times is the predicted transition time $\mathbf{f}_{j,i}(t)$ from Eq. **8**. Horizontal black line is the threshold that is moved from the top of the curve to 0 in 100 steps. Red vertical lines indicate that these transitions are coincident with the portion of the red curve that is above the threshold. (*Right*) The ROC curve for this example. Arrows indicate how one moves along the curve as the threshold moves. *AUC*: area under the ROC curve.